Available online at www.sciencedirect.com
ScienceDirect
Journal of Power Sources 161 (2006) 1281–1287
JOURNAL OF POWER SOURCES
www.elsevier.com/locate/jpowsour

Electrochemical properties of nano-sized Fe_2O_3-loaded carbon as a lithium battery anode

Bui Thi Hang [a,*], Izumi Watanabe [a], Takayuki Doi [b], Shigeto Okada [b], Jun-Ichi Yamaki [b]

[a] *Japan Science and Technology Agency, Kasuga Koen 6-1, Kasuga, Fukuoka 816-8580, Japan*
[b] *Institute for Materials Chemistry and Engineering, Kyushu University, Kasuga Koen 6-1, Kasuga, Fukuoka 816-8580, Japan*

Received 10 March 2006; received in revised form 5 June 2006; accepted 6 June 2006
Available online 12 July 2006

Abstract

Nano-sized Fe_2O_3-loaded carbon material was prepared by loading Fe_2O_3 on carbon using a chemical method. $Fe(NO_3)_3$ was impregnated on carbon in an aqueous solution, and the mixture was dried and then calcined for 1 h at 400 °C in flowing Ar. Transmission electron microscopy (TEM) coupled with X-ray diffraction measurements revealed that small Fe_2O_3 particles (a few tenths of nanometers) were distributed on the carbon surface. The obtained nano-sized Fe_2O_3-loaded carbon material acted as an anode in a Li cell. High charge capacities of over 1000 mAh g^{-1} (reduction of Fe_2O_3) in the first charge process suggested that Fe^{3+} in Fe_2O_3 was electrochemically reduced to Fe^0. Investigation of the charge material by X-ray photoelectron spectroscopy (XPS) confirmed that Fe^{3+} is reduced to Fe^0. Nano-sized Fe_2O_3-loaded acetylene black (AB), which, due to the larger surface area of AB, gave a greater distribution of nano-sized Fe_2O_3 particles than graphite, provided a larger capacity than nano-sized Fe_2O_3-loaded graphite.
© 2006 Elsevier B.V. All rights reserved.

Keywords: Nano-sized Fe_2O_3-loaded carbon material; Lithium battery anode

1. Introduction

Various kinds of alternative materials for lithium battery anodes and cathodes have been extensively studied. Transition metal oxides, in particular, have received much attention. The electrochemical reduction of these oxides in lithium cells has been studied thoroughly. Iron oxides, which are inexpensive and have low environmental impact, are potential candidates for use in lithium batteries. Many researchers have reported that iron oxides serve as an active material in lithium batteries [1–6]. Godshall et al. [6] indicated that lithium could react with iron oxides, to give Li_2O and metallic iron, through the intermediate formation of various phases such as $LiFe_5O_8$, $LiFeO_2$ and Li_5FeO_4. Larcher et al. [7] confirmed that α-Fe_2O_3 was reduced to form iron metal and Li_2O. Thus, the overall electrochemical reaction of lithium intercalation to iron oxides is as follows:

$$6Li^+ + Fe_2O_3 + 6e \rightarrow 2Fe + 3Li_2O \quad (1)$$

$$8Li^+ + Fe_3O_4 + 8e \rightarrow 3Fe + 4Li_2O \quad (2)$$

However, it has been considered that it is difficult to use large particles of iron oxides for a lithium secondary battery due to their irreversible phase transformation during the reaction [1–4]. Recently, some iron oxides with nano-sized particles have been reported to react with lithium as a reversible material [7–12]. Among these works, Larcher et al. [7,8] described the effect of particle size on lithium intercalation into α-Fe_2O_3 particles. Two electrodes that contain nanometric α-Fe_2O_3 and micrometric α-Fe_2O_3 particles were investigated and the results showed that high capacities (1400 and 1200 mAh g^{-1} for nano-α-Fe_2O_3, and micro-α-Fe_2O_3, respectively) could be obtained on the first discharge process (reduction of Fe_2O_3). Matsumura et al. [9] focused on a materials search, in which both lithium insertion and surface reactions proceed on the surface of small particles, to improve cell capacities. They synthesized a nano-sized α-Fe_2O_3/SnO_2 binary system (ca. 7 nm) with an SO_4^{2-} additive, and reported that a compound with $(\alpha\text{-}Fe_2O_3)_{0.7}$–$(SnO_2)_{0.3}$ shows a reversible capacity of 300 mAh g^{-1} based on lithium intercalation and the surface reaction on the particles. Moreover, other researchers [10–12] have shown that fine iron oxides (Fe_2O_3 or Fe_3O_4) provide large capacities for a lithium battery. Therefore, the particle size and surface area of iron oxide influence the cycle performance.

* Corresponding author. Tel.: +81 92 583 7790; fax: +81 92 583 7790.
E-mail address: hang@cm.kyushu-u.ac.jp (B.T. Hang).

0378-7753/$ – see front matter © 2006 Elsevier B.V. All rights reserved.
doi:10.1016/j.jpowsour.2006.06.002

Table 1
Main characteristics of the carbon materials

	Grain size (nm)	BET surface area ($m^2\ g^{-1}$)	True density ($g\ cm^{-3}$)
AB	40–100	68	2.0
Natural graphite	1 8000	8	2.24

To obtain fine iron oxide particles and increase the surface area of active material, in this study, acetylene black and graphite were used as a substrate to disperse iron oxides. For this purpose, two types of electrode materials, nano-sized Fe_2O_3/C mixed and nano-sized Fe_2O_3-loaded carbon, were prepared and used as an anode material for a lithium cell. The electrochemical activities of these materials with lithium were investigated and compared to find the most suitable material for a lithium battery anode.

2. Experimental

Acetylene black (AB, Denki Kagaku Co.) and natural graphite (Chuetsu Graphite Co.), with average diameters of ca. 100 nm and 18 μm, respectively, were used in the present work. The main characteristics of the carbon materials used are listed in Table 1; their morphology is showed in Fig. 1. Iron nitrate (Wako Pure Chemical Co.) was used as the iron source.

Nano-sized Fe_2O_3-loaded carbon material was prepared by loading Fe_2O_3 on carbon, as described below. $Fe(NO_3)_3$ was impregnated on carbon with an iron to carbon weight ratio of 1:8 in an aqueous solution, and the mixture was dried at 70 °C. This was followed by calcination for 1 h at 400 °C in flowing Ar. The iron compound obtained on the carbon materials was identified to be Fe_2O_3 by X-ray diffraction. The morphology of the as-prepared nano-sized Fe_2O_3-loaded carbon materials was observed by transmission electron microscopy (TEM) using a TECNAI F20. X-ray measurements were also carried out on these materials.

All electrochemical measurements were performed at 25 °C using a coin cell with lithium metal as a cathode. The anode was prepared by mixing 90 wt.% nano-sized Fe_2O_3-loaded carbon with 10 wt.% polyvinylidene fluoride (PVdF) binder (KF #9100 from Kureha Chemical) dissolved in 1-methyl-2-pyrrolidinone (NMP). The slurry was coated onto the copper current collector. The coated films were dried and cut to 15 mm in diameter. Nano-sized Fe_2O_3 electrodes without and with carbon were also prepared by the same procedure with 90 wt.% nano-sized Fe_2O_3 (Aldrich, ca. 3 nm) or nano-sized Fe_2O_3/C mixed and 10 wt.% PVdF binder for comparison with nano-sized Fe_2O_3-loaded carbon. These electrodes were then dried for 12 h at 120 °C in a vacuum oven. The cells were assembled in an argon-filled glove box. The electrolyte and separator used were: 1 M $LiPF_6$ in EC-DMC 1:1 by volume (Tomiyama Pure Chemical Co.) and porous polypropylene (Celgard #3501), respectively.

Cyclic voltammetry (CV) studies were carried out using an AutoLab instrument (ECO CHEMIE) at a scanning rate of $0.5\ mV\ s^{-1}$. Charge–discharge cycle tests of the coin cells were conducted at a constant current density of $0.2\ mA\ cm^{-2}$ and within a voltage range of 0.5–3.0 V (versus Li/Li^+) using a cell-cycling device (NAGANO Co.).

To obtain the valence state of iron before and after cycling, X-ray photoelectron spectroscopy (XPS) analysis (JPS-9010 MC/IV, JOEL) was performed. After cycling, the coin cells were disassembled in a glove box filled with argon, and the working electrodes were washed with DMC solvent and then dried in a vacuum for 12 h. These electrodes were moved for XPS measurement by using a transfer vessel. The X-ray source was a monochromatic Mg K_α radiation system (10 kV, 10 mA).

3. Results and discussion

The X-ray pattern of the as-prepared material using AB is presented in Fig. 2. Fe_2O_3 is indeed present on the carbon surface. Therefore, the active material in this case is Fe_2O_3.

For the preparation condition, the weight ratio of iron to carbon is 1:8. In order to determine the real iron amount existed in the final production, the polarized zeeman atomic absorption spectrophotometer (PZAAS) method was applied. The as-prepared material was immersed in chloride acid solution to dissolve iron oxide. The obtained solution was checked by PZAAS and the results are showed in Table 2. It appears that the iron amount in the final production is a little bit smaller than that in preparation condition. Thereby, the real weight ratio of iron to carbon in the obtained Fe_2O_3-loaded carbons is about 1:9.

To confirm the nature of the Fe_2O_3 present on the carbons, TEM measurements were carried out. TEM images of

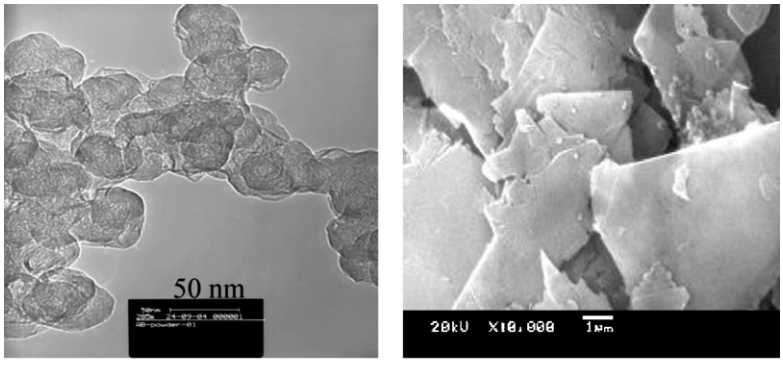

AB Natural graphite

Fig. 1. Morphology of the carbon materials.

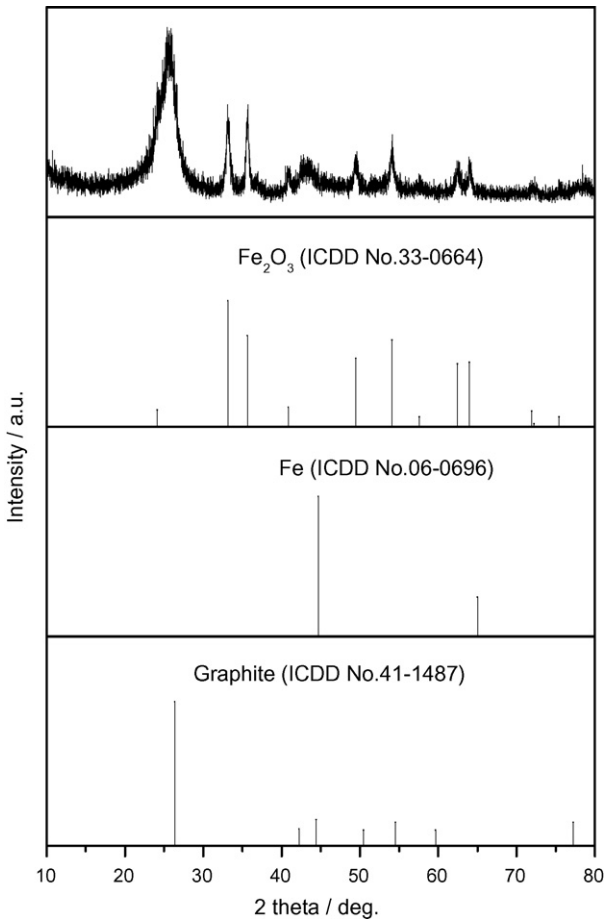

Fig. 2. X-ray pattern of the as-prepared nano-sized Fe_2O_3-loaded AB.

Table 2
PZAAS result for nano-sized Fe_2O_3-loaded carbon (Fe:C = 1:8 in preparation condition)

Fe_2O_3-loaded carbon	Iron amount in preparation condition (mg)	Iron amount obtained from measurement (mg)	Weight ratio obtained from measurement (Fe:C)
AB	11.1177	9.7972	~1:9
Natural graphite	11.1144	9.7936	~1:9

as-prepared Fe_2O_3-loaded carbons are shown in Fig. 3. The dark particles in this figure are Fe_2O_3. The TEM images demonstrated that fine Fe_2O_3 particles (a few tenths of nanometers) were dispersed on the carbon surface. Such dispersion should increase the surface area of active material and improve the redox reaction of iron.

Fig. 4 shows cyclic voltammograms for nano-sized Fe_2O_3-loaded AB and graphite in the five initial cycles. The CV curves for both electrodes clearly indicated a reversible reaction during reduction and oxidation with two peaks at around 1.5 and 0.7 V (versus Li/Li^+) in reduction and one peak at around 1.8 V (versus Li/Li^+) in oxidation. Similar CV profiles obtained with nano-sized Fe_2O_3/AB and nano-sized Fe_2O_3/graphite mixed electrodes are shown in Fig. 5. However, the redox current for the nano-sized Fe_2O_3 mixed with carbon electrodes decreased rapidly with repeated cycling.

Comparison of the CV results with nano-sized Fe_2O_3-loaded carbon (Fig. 4) and nano-sized Fe_2O_3/C mixed (Fig. 5) electrodes with the CV results of nano-sized Fe_2O_3 (Aldrich, ca. 3 nm) without carbon (Fig. 6) demonstrated that nano-sized Fe_2O_3-loaded carbon materials exhibited better reversible capacity than nano-sized Fe_2O_3 without carbon as well as nano-sized Fe_2O_3/C mixed electrodes. From these profiles, it can be seen that nano-sized Fe_2O_3-loaded carbon acts as a rechargeable electrode material in a lithium battery. However, the currents gradually decreased during cycling, which means that the capacities of these electrodes also gradually decreased with an increase in the number of charge–discharge cycles.

Figs. 7 and 8 show the charge and discharge curves in the initial 10 cycles for nano-sized Fe_2O_3, nano-sized Fe_2O_3 mixed with carbon and nano-sized Fe_2O_3-loaded carbon electrodes between 0.5 and 3.0 V. All of the electrodes showed a large irreversible capacity in the first cycle. Nano-sized Fe_2O_3 electrode without carbon exhibited poor cyclability while nano-sized Fe_2O_3-loaded carbon electrode provided excellent cycle performance. Although nano-sized Fe_2O_3/C mixed electrodes delivered better cyclability than nano-sized Fe_2O_3 electrodes without carbon, they still showed a large capacity loss upon repeated cycling. Thus, among the electrodes used, nano-sized Fe_2O_3-loaded carbon gave the best results, which are consistent with the CV results.

For nano-sized Fe_2O_3-loaded carbon, when AB was used (Fig. 8b), the electrode exhibited a high charge capacity

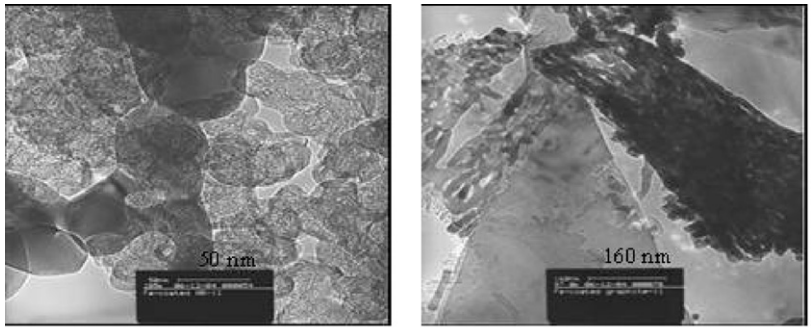

Fig. 3. TEM images of the as-prepared nano-sized Fe_2O_3-loaded carbon materials.

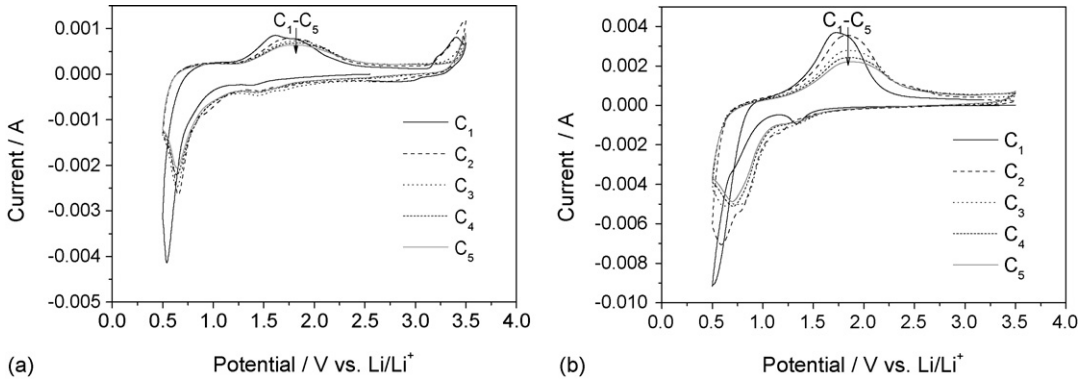

Fig. 4. Cyclic voltammograms for (a) nano-sized Fe_2O_3-loaded AB and (b) nano-sized Fe_2O_3-loaded graphite in the five initial cycles. Scan rate 0.5 mV s^{-1}.

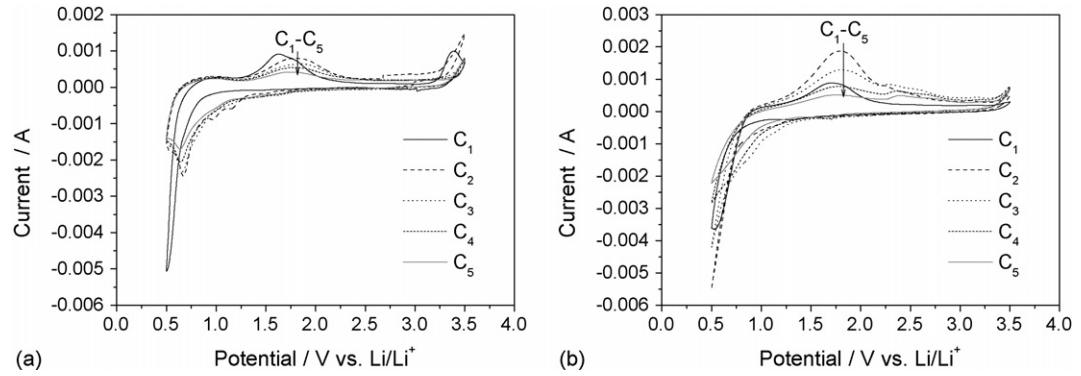

Fig. 5. Cyclic voltammograms for (a) nano-sized Fe_2O_3/AB mixed and (b) nano-sized Fe_2O_3/graphite mixed electrode in the five initial cycles. Scan rate 0.5 mV s^{-1}.

of about 2600 mAh g^{-1} (reduction of Fe_2O_3) while the discharge capacity reached about 1600 mAh g^{-1} (oxidation of iron) in the first cycle. In the case of nano-sized Fe_2O_3-loaded graphite (Fig. 8(d)), in the first cycle the electrode also provided high charge and discharge capacities of about 1200 and 800 mAh g^{-1}, respectively. Therefore, both electrode materials exhibited higher charge and discharge capacities in the first cycle than those reported in previous works [8–10,12]. This result may be due to the large surface area of nano-sized Fe_2O_3 distributed on the carbon surface prepared by loading nano-sized Fe_2O_3 particles on a carbon surface using a chemical method. However, a large irreversible capacity was observed in the first cycle to give a coulombic efficiency of over 60% for both electrodes. In addition, the capacity gradually degraded during the charge–discharge process. A possible reason for the large irreversible capacity and capacity degradation may be the reaction of electrolyte to form a solid electrolyte interface (SEI) layer at the electrode surface. Another possibility may be the re-contribution of iron species on the carbon surface during cycling. The theoretical capacity calculated from Eq. (1) is 1006 mAh g^{-1}, which

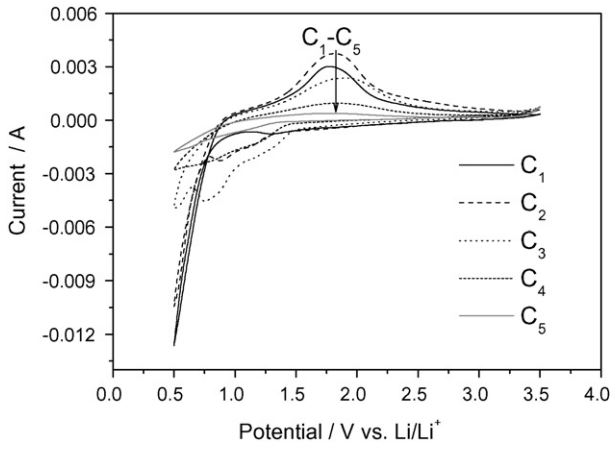

Fig. 6. Cyclic voltammograms for nano-sized Fe_2O_3 (Aldrich) without carbon in the five initial cycles. Scan rate 0.5 mV s^{-1}.

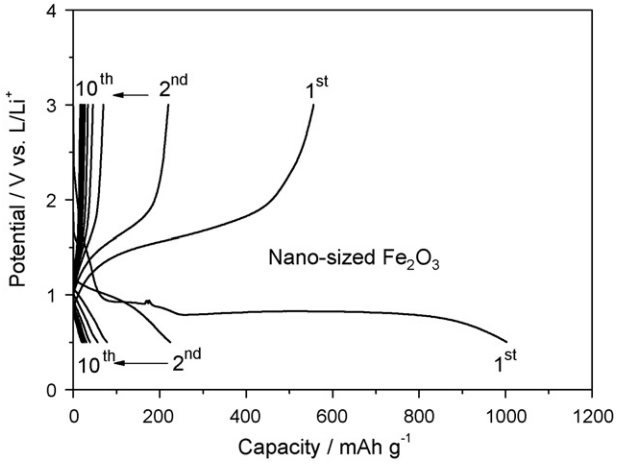

Fig. 7. Charge–discharge curves in the 10 initial cycles for nano-sized Fe_2O_3 at 0.2 mA cm^{-2}.

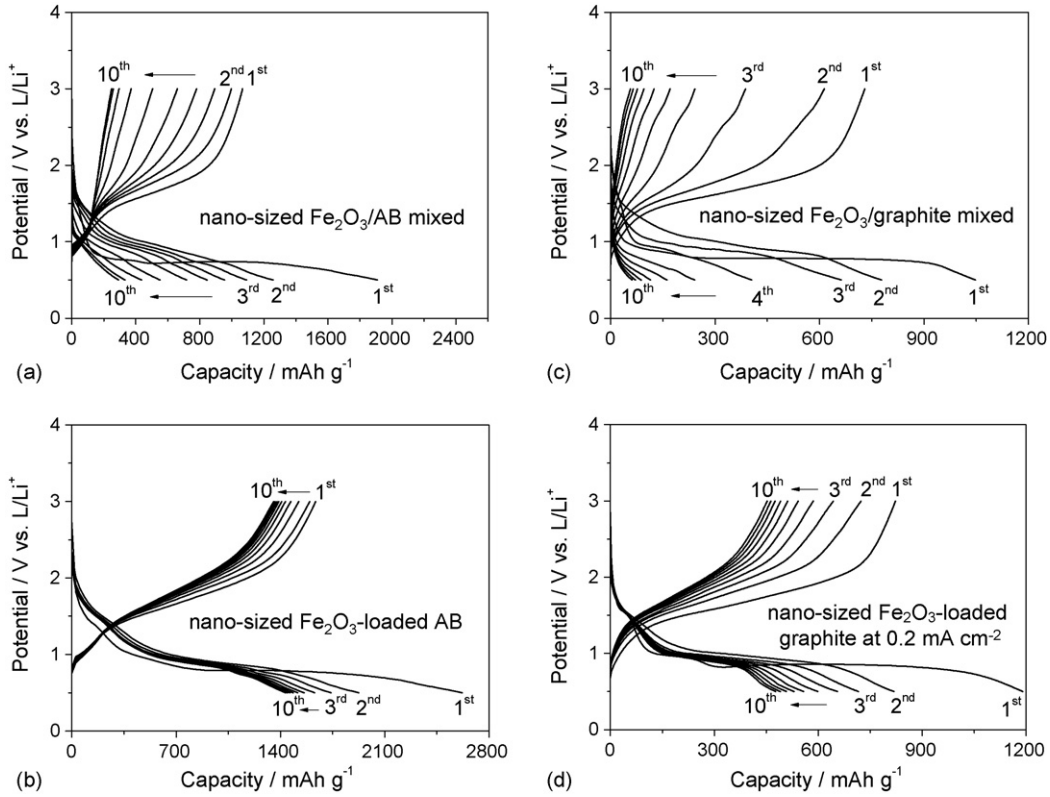

Fig. 8. Charge–discharge curves in the 10 initial cycles for (a) nano-sized Fe_2O_3/AB mixed, (b) nano-sized Fe_2O_3-loaded AB, (c) nano-sized Fe_2O_3/graphite mixed and (d) nano-sized Fe_2O_3-loaded graphite at 0.2 mA cm^{-2}.

corresponds to six Li per Fe_2O_3. The large observed excess capacity in both electrodes suggests that all of the Fe^{3+} was reduced to Fe^0 via an electrochemical reaction and the electrolyte underwent a reaction.

To check the valence state of iron before and after the first charge process, XPS measurements were carried out and the results are presented in Figs. 9 and 10. Before cycling (Fig. 9), for both electrodes, the sharp peak of the Fe $2p_{3/2}$ component at a binding energy of 710.9 eV is characteristic of trivalent iron (Fe_2O_3) [13]. After the first charge process (reduction of Fe_2O_3), the Fe $2p_{3/2}$ peak was shifted toward a lower binding energy at around 706.9 eV (Fig. 10). The position of this peak is consistent with iron metal reported in the Handbook of XPS [13]. This result indicates that during the charge process, trivalent iron is reduced to iron metal.

Fig. 11 compares the charge–discharge capacities to the cycle numbers for nano-sized Fe_2O_3-loaded AB and graphite, respectively. Both electrode materials showed large reversible capacities in the initial 20 cycles. However, the capacities then gradually decreased and achieved stable values. Carbon materials also contributed to the capacity of the electrode. Larcher et al. [8] showed that the reaction of lithium with carbon SP is about 60 mAh g^{-1}, which is small compared to the high capacity values in their work. To determine the contribution of carbon, in the present study, a carbon electrode without Fe_2O_3 was cycled and the results are shown in Fig. 11. These results confirmed

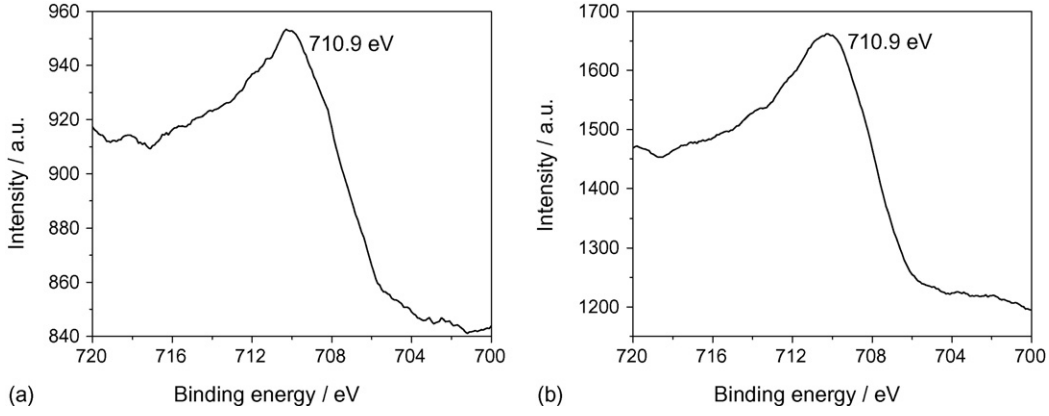

Fig. 9. XPS spectra of Fe $2p_{3/2}$ core level for (a) nano-sized Fe_2O_3-loaded AB and (b) nano-sized Fe_2O_3-loaded graphite before cycling.

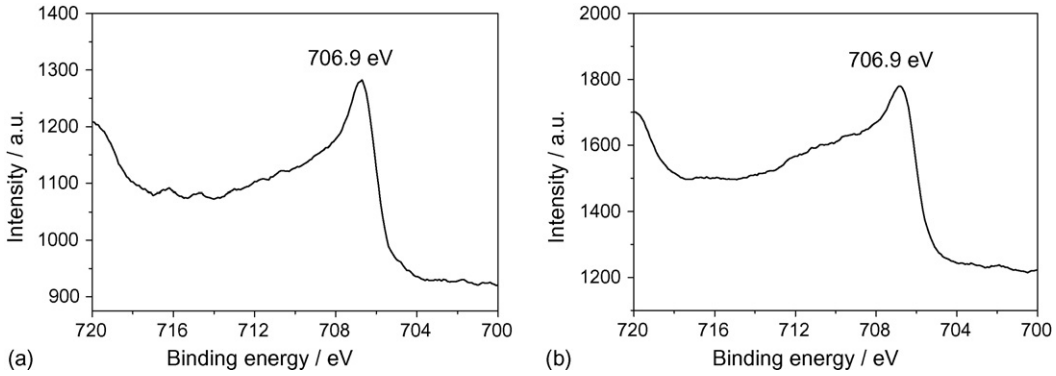

Fig. 10. XPS spectra of Fe $2p_{3/2}$ core level for (a) nano-sized Fe_2O_3-loaded AB and (b) nano-sized Fe_2O_3-loaded graphite after the first charge (reduction of Fe_2O_3).

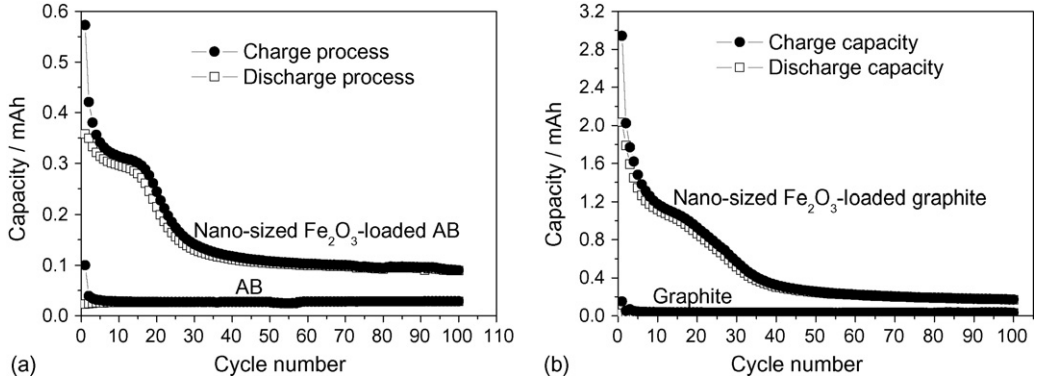

Fig. 11. Cycle performance of (a) AB and nano-sized Fe_2O_3-loaded AB and (b) graphite and nano-sized Fe_2O_3-loaded graphite.

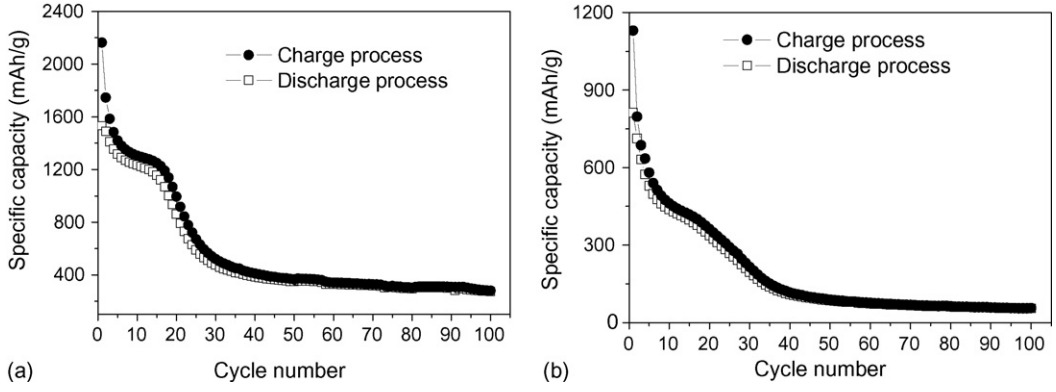

Fig. 12. Cycle performance of (a) nano-sized Fe_2O_3-loaded AB and (b) nano-sized Fe_2O_3-loaded graphite.

that the capacity caused by the reaction of lithium with carbon is very small compared to that of nano-sized Fe_2O_3-loaded carbon electrodes. However, for both nano-sized Fe_2O_3-loaded AB and graphite electrodes (Fig. 12), the stable specific capacities obtained are relatively small compared with those seen in the initial cycles. As mentioned above, this may be due to the decomposition of electrolyte to form an SEI layer at the electrode surface and/or the re-distribution of iron species during cycling to result in a large capacity loss. Another possible explanation may involve the large difference in particle size between nano-sized Fe_2O_3 (a few tenths of nanometers) and carbon (Table 1) [12]. A direct comparison of nano-sized Fe_2O_3-loaded AB and graphite shows that the reversible capacity values of nano-sized Fe_2O_3-loaded AB are greater than those of nano-sized Fe_2O_3-loaded graphite. This phenomenon can be explained based on the difference in the distribution of iron oxide on the carbon surface. In the case of AB, which has a greater surface area than graphite (see Table 1), iron oxide particles are more dispersed than on graphite, resulting in a greater surface area of iron oxide on AB than on graphite. Thereby, nano-sized Fe_2O_3-loaded AB provided a higher capacity than nano-sized Fe_2O_3-loaded graphite.

4. Conclusion

Nano-sized Fe_2O_3-loaded carbon materials using AB and graphite were successfully prepared by a chemical method.

Nano-sized Fe_2O_3-loaded AB and graphite act as rechargeable electrode materials in a lithium cell. The high capacities observed for both electrodes suggest that Fe^{3+} in Fe_2O_3 was reduced to Fe^0 via electrochemical reactions. Although a large capacity loss occurred with both electrode materials, nano-sized Fe_2O_3-loaded AB is a more promising candidate than graphite as an electrode material for a lithium battery anode. With further improvements in capacity retention, nano-sized Fe_2O_3-loaded AB is expected to be a potential candidate for use at the anode to achieve high capacity in a lithium battery.

Acknowledgement

This work was supported by the CREST program of JST (Japan Science & Technology Agency).

References

[1] M.M. Thackeray, J. Coetzer, Mater. Res. Bull. 16 (1881) 591–597.
[2] M.M. Thackeray, W.I.F. David, J.B. Goodenough, Mater. Res. Bull. 17 (1882) 785–793.
[3] M.M. Thackeray, W.I.F. David, J.B. Goodenough, J. Solid State Chem. 55 (1984) 280–286.
[4] M. Pernet, P. Strobel, B. Bonnet, P. Bordet, Y. Chabre, Solid State Ionics 66 (1993) 259–265.
[5] B.D. Pietro, M. Patriarca, B. Scrosati, J. Power Sources 8 (1982) 289–299.
[6] N.A. Godshall, I.D. Raistrick, R.A. Huggins, Mater. Res. Bull. 15 (1980) 561.
[7] D. Larcher, D. Bonnin, R. Cortes, I. Rivals, L. Personnaz, J.M. Tarascon, J. Electrochem. Soc. 150 (2003) A1643–A1650.
[8] D. Larcher, C. Masquelier, D. Bonnin, Y. Chabre, V. Masson, J.B. Leriche, J.M. Tarascon, J. Electrochem. Soc. 150 (2003) A133–A139.
[9] T. Matsumura, N. Sonoyama, R. Kanno, M. Takano, Solid State Ionics 158 (2003) 253–260.
[10] H. Morimoto, S. Tobishima, Y. Iizuka, J. Power Sources 146 (2005) 315–318.
[11] S. Ito, K. Nakaoka, M. Kawamura, K. Ui, K. Fujimoto, N. Koura, J. Power Sources 146 (2005) 319–322.
[12] S. Kanzaki, T. Inada, T. Matsumura, N. Sonoyama, A. Yamada, M. Takano, R. Kanno, J. Power Sources 146 (2005) 323–326.
[13] Handbook of XPS (JEOL).